

Diagnostic guidance for patients with persistent pulmonary abnormalities after COVID-19 infection: the potential benefit of 68Ga-FAPI PET/CT

Anna Sviridenko (✉ anna.sviridenko@tirol-kliniken.at)

Medizinische Universität Innsbruck: Medizinische Universität Innsbruck <https://orcid.org/0000-0002-7312-7657>

Anna Boehm

Medizinische Universität Innsbruck Department Innere Medizin

Gianpaolo Di Santo

Medical University Innsbruck Department of Radiology: Medizinische Universität Innsbruck Department Radiologie

Christian Uprimny

Medical University of Innsbruck: Medizinische Universität Innsbruck

Bernhard Nilica

Medical University of Innsbruck: Medizinische Universität Innsbruck

Josef Fritz

Medical University of Innsbruck: Medizinische Universität Innsbruck

Frederik L. Giesel

University Hospital Heidelberg: UniversitätsKlinikum Heidelberg

Uwe Haberkorn

University Hospital Heidelberg: UniversitätsKlinikum Heidelberg

Sabina Sahanic

Medizinische Universität Innsbruck: Medizinische Universität Innsbruck

Clemens Decristoforo

Medical University of Innsbruck: Medizinische Universität Innsbruck

Ivan Tancevski

Medizinische Universität Innsbruck: Medizinische Universität Innsbruck

Gerlig Widmann

Medical University Innsbruck Department of Radiology: Medizinische Universität Innsbruck Department Radiologie

Judith Loeffler-Ragg

Medical University of Innsbruck: Medizinische Universität Innsbruck

Irene Virgolini

Medical University of Innsbruck: Medizinische Universität Innsbruck

Short Report

Keywords: SARS-CoV-2, 68Ga-FAPI-46 PET/CT, 18F-FDG PET/CT, idiopathic pulmonary fibrosis

Posted Date: April 12th, 2022

DOI: <https://doi.org/10.21203/rs.3.rs-1514819/v1>

License:  This work is licensed under a Creative Commons Attribution 4.0 International License.

[Read Full License](#)

Abstract

Coronavirus disease 2019 (COVID-19)-related pneumonia challenges clinical practice. We explore the potential diagnostic benefit of positron emission tomography/computed tomography (PET/CT) in order to establish the underlying inflammatory or fibrotic repair processes in prolonged structural lung abnormalities in COVID-19 patients.

Methods: Six post-COVID-19 patients suspected for pulmonary fibrosis were scheduled for dual tracer PET/CT with ^{18}F -FDG (fluorodeoxyglucose) and ^{68}Ga -fibroblast activation protein inhibitor (FAPI)-46. The uptake of ^{68}Ga FAPI-46 in the involved lung was compared to a control group of nine non COVID-19 patients. Clinical data and PET/CT imaging were collected and analysed.

Results: PET/CT revealed in all six pulmonary impaired patients the reduced glucose avidity on ^{18}F -FDG and clear positivity on ^{68}Ga -FAPI-46 PET/CT in comparison to the control group.

Conclusion: Indicating fibrotic repair mechanisms, ^{68}Ga -FAPI PET/CT may enhance non-invasive clinical diagnostic performance, drive therapeutic interventions, and facilitate therapeutic response monitoring in patients with long-term CT-abnormalities after severe COVID-19.

Introduction

In some individuals after a severe course of COVID-19 the pulmonary injury appears to persist [1, 2, and 3].

Whether those prolonged structural lung abnormalities in COVID-19 patients are mainly triggered by underlying inflammatory or fibrotic repair processes has not yet been answered.

Within incidental acute SARS-CoV-2 ^{18}F -FDG-PET/CT already proved to discriminate between morpho-metabolic patterns reflecting the evolutionary phases of inflammatory processes [4]. However, the role of ^{18}F -FDG-PET/CT within the diagnostic pathway of long-term pulmonary changes after SARS-CoV-2 infection remains elusive.

The FAP (fibroblast activation protein) expresses on fibroblasts during tissue remodelling, tissue repair and carcinogenesis [5, 6]. Moreover, FAP is selectively induced in activated fibroblasts in a murine model of pulmonary fibrosis [7, 8].

Recently, ^{68}Ga -FAPI PET/CT could visualize tracer uptake in several cancers and in fibrotic lesions exemplary in idiopathic pulmonary fibrosis (IPF) [9–11].

Materials And Methods

Subjects and study design:

Between October 2020 and June 2021 six patients with a confirmed diagnosis of COVID-19 participated in the prospective CovILD study. The trial protocol was approved by the institutional review board at Innsbruck Medical University (EK Nr: 1103/2020) and was registered at ClinicalTrials.gov (registration number NCT04416100). Informed consent was obtained from each patient. The inclusion criteria were 1) post-COVID-19 positive cases; 2) patients with objectively persisting dyspnea; 3) patients underwent thin-section chest CT (computer tomography) scans at least twice during the hospitalization and had at least one follow-up CT after discharge with the evidence of persistent lung abnormalities; 4) patients with both ¹⁸F-FDG PET/CT and ⁶⁸Ga-FAPI PET/CT scan after discharge.

Detailed characteristics of the patient's post-COVID 19 cohort are shown in Table 1.

Table 1
Demographics and clinical characteristics of enrolled post-COVID-19 patients.

Patient no.	Sex	Age (y)	Time from the COVID positivity to PET/CT (days)	Treatment during infection	Time from ⁶⁸ Ga-FAPI to ¹⁸ F-FDG PET/CT (days)
1	F	71	177	Oxygen supply	10
2	M	57	229	Invasive ventilation	14
3	M	79	203	Oxygen supply	13
4	M	70	181	Invasive ventilation	8
5	M	54	193	Invasive ventilation	14
6	M	49	147	Invasive ventilation	13

Nine oncological patients with different extrapulmonary tumor entities underwent ⁶⁸Ga-FAPI PET/CT were included as control group of non COVID-19 patients.

Radiopharmaceutical preparation:

⁶⁸Ga-FAPI 46 was prepared in a procedure similar to that recently described [14]

CT and PET/CT imaging:

All patients underwent a previous (performed within 30 days before PET/CT) thin-section chest CT scan on a 1280 slice multidetector CT with a 128x0,6 mm collimation and spiral pitch factor of 1.1 (SOMATOM Definition Flash, Siemens Healthineers).

The PET/CT imaging was conducted according to the lastly published Declaration of Helsinki [13]. All PET/CT scans were performed on a dedicated PET/CT system (Discovery DMI; GE Healthcare,

Milwaukee, WI, USA). All patients were first scheduled for ^{68}Ga -FAPI PET/CT and followed by ^{18}F -FDG PET/CT within 14 days.

[^{68}Ga] FAPI – 46 PET imaging:

The acquisition protocol for ^{68}Ga -FAPI PET/CT included a dynamic scan with 12 images with 10 seconds and 36 images with 30 seconds positioned over the lungs and whole-body scans (skull base to upper thighs) in three-dimensional mode. Emission time was 2 minutes per bed position, the axial field of view: 20 cm per bed position.

A mean dosage of 220 ± 34 MBq ^{68}Ga -FAPI was administered intravenously, dynamic image acquisition at injection time and static image acquisition after 30, 60 and 120 minutes post injection were performed. PET reconstructions were performed with the ordered subset expectation maximization algorithm (OSEM) Q.Clear® (GE Healthcare) with a β of 1000.

A low-dose CT scan was performed for attenuation correction of the PET emission data. The low-dose CT scan parameters using smart mA dose modulation were: 100 kVp, 20–100 mA, noise index 51, 0.5 s per tube rotation, slice thickness 3.75 mm and pitch 0.98.

^{18}F -FDG PET imaging:

For ^{18}F -FDG PET/CT an acquisition protocol according to the guidelines of the European Association of Nuclear Medicine was applied [14]. In all patients a low-dose CT from the skull vertex to mid-thigh was obtained first, using the same parameters as described for ^{68}Ga -FAPI PET.

Image Analysis

First, a visual assessment for elevated trace uptake (higher than mediastinal blood pool) was performed.

For semiquantitative analysis the maximal standardized uptake value (SUVmax) and target-to-background ratio (TBR) were calculated. Volume of interest (VOIs) were drawn on the axial PET image to measure the SUVmax and SUV mean values, we based on the suspected fibrotic area at high resolution CT. TBR was calculated by dividing the SUVmax of the fibrotic area by the SUV mean of the blood pool (15 mm spherical VOI in the center of right atrium)

We calculated SUVmax and TBR of ^{68}Ga -FAPI after 30, 60 and 120 minutes together with SUV max and TBR of ^{18}F -FDG scans of pulmonary impaired patients. Furthermore SUVmax and TBR values of the ^{68}Ga -FAPI control group non COVID 19 patients were evaluated. The FAPI SUVmax and TBR after 60 minutes values of the pulmonary impaired post COVID-19 patient group were compared with corresponding values in the control group. In addition, the correlation between the FAPI parameters after 60 minutes and the FDG equivalents in the pulmonary impaired post COVID-19 patient group were analyzed.

The dynamic PET images were used to analyze the ^{68}Ga -FAPI uptake in aorta (bloodpool) and fibrotic areas. Therefore VOIs for aorta and fibrotic areas were drawn in selected slices and diagrams with

activity VOI content over acquisition time were derived.

The times to peak value (minutes from the beginning of the dynamic acquisition to the maximum of SUV_{max} of the lesion) were derived from the time–activity curves.

Statistical Analysis

TBR and SUV_{max} values of FDG PET/CT and ⁶⁸Ga-FAPI were analyzed descriptively reporting means and standard deviations (SDs). Moreover, the independent samples t-test was applied to compare the ⁶⁸Ga-FAPI PET values of the pulmonary impaired patient group with the control group. The same test was applied to compare the ⁶⁸Ga-FAPI and ¹⁸F-FDG values within the pulmonary impaired patient group. Comparisons across different time-points (within the pulmonary impaired patient group) were performed using paired samples t-tests. All statistical tests were two-sided at a significance level of 0.05. Statistical analyses were conducted in SPSS, version 26.0 (IBM Corp., Armonk, NY, USA).

Results

PET/CT imaging showed positive ⁶⁸Ga-FAPI uptake in all suspected fibrotic areas of post COVID-19 patients.

In static ⁶⁸Ga-FAPI imaging the suspected pulmonary abnormalities in post COVID-19 patients showed for ⁶⁸Ga-FAPI a mean SUV_{max} of 3.81 ± 1.24 after 30 minutes, 2.75 ± 0.32 after 30 minutes and 2.74 ± 0.31 after 60 minutes, respectively; the mean TBR Ratio was 1.65 ± 0.50 after 30 minutes, 2.05 ± 0.28 after 60 minutes and 1.29 ± 0.32 after 120 minutes, respectively.

We have found significantly higher TBR of ⁶⁸Ga-FAPI after 60 minutes in respect to TBR after 120 minutes (P value = 0.003)

The estimated mean SUV_{max} of ⁶⁸Ga-FAPI within the pulmonary parenchyma in the control group was 1.04 ± 0.25 and the TBR 0.74 ± 0.15 , both after 60 minutes.

The ⁶⁸Ga-FAPI PET scans depicted significantly increased SUV_{max} and TBR values in the pulmonary impaired post COVID patient group compared with the control group (P values for both parameters < 0.001)

In contrast to ⁶⁸Ga-FAPI, ¹⁸F-FDG PET/CT imaging was visually negative on all patients.

In relation to the glucose metabolical characterization of pulmonary lesions the calculated SUV_{max} and TBR of ¹⁸F-FDG PET were 2.05 ± 0.28 and 0.65 ± 0.12 , respectively.

Furthermore, the ⁶⁸Ga-FAPI PET obtained after 60 minutes revealed significantly higher tracer uptake in term of SUV_{max} and TBR in residual fibrotic lesions in comparison to ¹⁸F-FDG PET/CT (P value = 0.003 and < 0.001, respectively). A depictive case is shown in Fig. 1.

The ^{68}Ga -FAPI time–activity curves for lung abnormalities showed an early peak just after median 40 s (range 27–90 s post administration) correlating with the aortic perfusion peak after 20 s (range 13–90) and 25% clearance blood pool after 212 s (range 139–333), followed by a slowly decreasing signal intensity in lung lesions over time.

Discussion

Accordingly, early lung function analysis of patients with COVID-19 at the time of discharge from hospital revealed a high rate of abnormalities indicative of potential interstitial lung disease [15].

The load of fibrotic lung disease following SARS-CoV-2 infection is tending to be high, the global load of fibrotic lung disease will apparently increase remarkably [16].

The early identification of patients at higher risk of lung injury and fibrotic damage is critical and therefore the necessity of diagnostic guidance for patients with persistent pulmonary abnormalities after COVID-19 infection appears to be eminent. The final origin of fibrotic findings in the lungs remains unknown: the viral infection, the secondary cytokine cascade, related to treatment or ventilation, or a mixture of all these factors come into consideration [16].

The diagnosis of pulmonary fibrosis based on CT findings remains challenging: parenchymal bands, irregular interfaces, reticular opacities, and traction bronchiectasis with or without honeycombing not always clearly present on the follow-up CT scans [17]. Unfortunately the histological confirmation appears also oft *not executable* or infeasible. Non-invasive clinical diagnostic performance is extremely advisable.

We intended to explore the potential diagnostic benefit of nuclear imaging in terms of PET/CT scanning in further characterization of impaired pulmonary convalescence.

Since the ^{18}F -FDG-PET/CT was negative and because no improvement on high-dose corticosteroids could be observed, we then assumed the presence of underlying fibrotic repair processes. This hypothesis is backed by former studies, which investigated the diagnostic yield of ^{68}Ga -FAPI PET/CT in lung cancer and IPF. The respective PET/CT analysis showed a low physiological background signal of FAP in tumour surrounding tissue, while increased tracer uptake in IPF-related fibrotic lesions was observed [7, 8 and 18]. Furthermore, the calculated SUVmax of ^{68}Ga -FAPI within the fibrotic lesions was similar to the calculated SUVmax of the here presented post-Covid-19 lesions [19].

Within IgG4-related disease, ^{68}Ga -FAPI PET/CT was able to discriminate between inflammatory and fibrotic activity [18].

Moreover, several trials (NCT04541680, NCT04619680, and NCT04607928) currently investigate the use of antifibrotic medication in COVID-19.

Conclusion

^{68}Ga -FAPI 46 PET/CT may enhance non-invasive clinical diagnostic performance in patients with long-term pulmonary CT abnormalities after severe SARS-CoV-2 infection by uncovering early fibrotic changes following severe respiratory infections such as COVID-19. Moreover, it may further drive therapeutic interventions by providing a rationale for antifibrotic treatment initiation in post COVID-19 patients. Nevertheless further studies are required in the direction of therapeutic response monitoring.

Declarations

Funding

This case series did not receive any funding. The authors have no relevant financial or non-financial interests to disclose.

Competing Interest

FLG is advisor at ABX, SOFIE Bioscience, Telix pharmaceutical.

FLG and UH have a patent application for quinolone based FAP-targeting agents for imaging and therapy in nuclear medicine and also have shares of a consultancy-group for iTheranostics.

No conflict of interests exist for AB, HS, TS, SS, AL, AP, CD, GW, IT, GW, IV, JLR.

Author Contributions

This study was performed in line with the principles of the Declaration of Helsinki. Approval was granted by the Ethics Committee of Medical University Innsbruck (EK Nr: 1103/2020)

References

1. Ng CK, Chan JW, Kwan TL, et al. Six month radiological and physiological outcomes in severe acute respiratory syndrome (SARS) survivors. *Thorax*. 2004;59:889–91. doi:10.1136/thx.2004.023762.
2. Mo X, Jian W, Su Z, et al. Abnormal pulmonary function in COVID-19 patients at time of hospital discharge. *Eur Respir J*. 2020;55(6):2001217.
3. Pogatchnik BP, Swenson KE, Sharifi H, et al. Radiology-pathology correlation in recovered COVID-19, demonstrating organizing pneumonia. *Am J Respir Crit Care Med*. 2020;202(4):598–9.
4. Ajuria-Illarramendi O, Martinez-Lorca A, Del P Orduña-Diez. M. [18F] FDG-PET/CT in different COVID-19 phases. *ID Cases*. 2020;21:e00869.
5. Park JE, Lenter MC, Zimmermann RN, Garin-Chesa P, Old LJ, Rettig WJ. Fibroblast activation protein, a dual specificity serine protease expressed in reactive human tumor stromal fibroblasts. *J Biol Chem*. 1999;274(51):36505–12. doi:10.1074/jbc.274.51.36505.

6. Loktev A, Lindner T, Burger EM, et al. Development of Fibroblast Activation Protein-Targeted Radiotracers with Improved Tumor Retention. *J Nucl Med*. 2019;60(10):1421–9.
7. Siveke JT. Fibroblast-Activating Protein: Targeting the Roots of the Tumor Microenvironment. *J Nucl Med*. 2018;59(9):1412–4.
8. Egger C, Cannet C, Gérard C, et al. Effects of the fibroblast activation protein inhibitor, PT100, in a murine model of pulmonary fibrosis. *Eur J Pharmacol*. 2017;809:64–72.
9. Varasteh Z, Mohanta S, Robu S, et al. Molecular imaging of fibroblast activity after myocardial infarction using a ⁶⁸Ga-labelled fibroblast activation protein inhibitor FAPI-04. *J Nucl Med*. 2019;60:1743–9.
10. Kratochwil C, Flechsig P, Lindner T, et al. ⁶⁸Ga-FAPI PET/CT: Tracer Uptake in 28 Different Kinds of Cancer. *J Nucl Med*. 2019;60(6):801–5.
11. Giesel FL, Heussel CP, Lindner T, et al. FAPI-PET/CT improves staging in a lung cancer patient with cerebral metastasis. *Eur J Nucl Med Mol Imaging*. 2019;46(8):1754–5.
12. Fully-automated production of [(⁶⁸Ga)Ga]-FAPI-46 for clinical application. Spreckelmeyer. Balzer S, Poetzsch M, Brenner S. *W. EJNMMI Radiopharm Chem*. 2020 Dec 17;5(1):31. doi: 10.1186/s41181-020-00112-x. PMID: 33331982.
13. World Medical Association. World Medical Association Declaration of Helsinki: ethical principles for medical research involving human subjects. *JAMA*. 2013;310(20):2191–4. doi:10.1001/jama.2013.281053.
14. Boellaard R, Delgado-Bolton R, Oyen WJ, et al. FDG PET/CT: EANM procedure guidelines for tumour imaging: version 2.0. *Eur J Nucl Med Mol Imaging*. 2015;42(2):328–54. doi:10.1007/s00259-014-2961-x.
15. Rees EM, Nightingale ES, Jafari Y, et al. COVID-19 length of hospital stay: a systematic review and data synthesis. *BMC Med*. 2020;18:270. doi:10.1186/s12916-020-01726-3.
16. George PM, Wells AU, Jenkins RG. Pulmonary fibrosis and COVID-19: the potential role for antifibrotic therapy. *Lancet Respir Med*. 2020 Aug;8(8):807–15.
17. Wang Y, Dong C, Hu Y, et al. Temporal Changes of CT Findings in 90 Patients with COVID-19 Pneumonia: A Longitudinal Study. *Radiology*. 2020;296(2):E55–64. doi:10.1148/radiol.2020200843.
18. Schmidkonz C, Rauber S, Atzinger A, et al. Disentangling inflammatory from fibrotic disease activity by fibroblast activation protein imaging. *Ann Rheum Dis*. 2020;79(11):1485–91.
19. Röhrich M, Leitz D, Flechsig P, et al. Fibroblast Activation Protein - specific PET/CT imaging in Idiopathic Pulmonary Fibrosis with Lung Cancer. *J Nucl Med*. 2019;60(suppl 1):298.

Figures

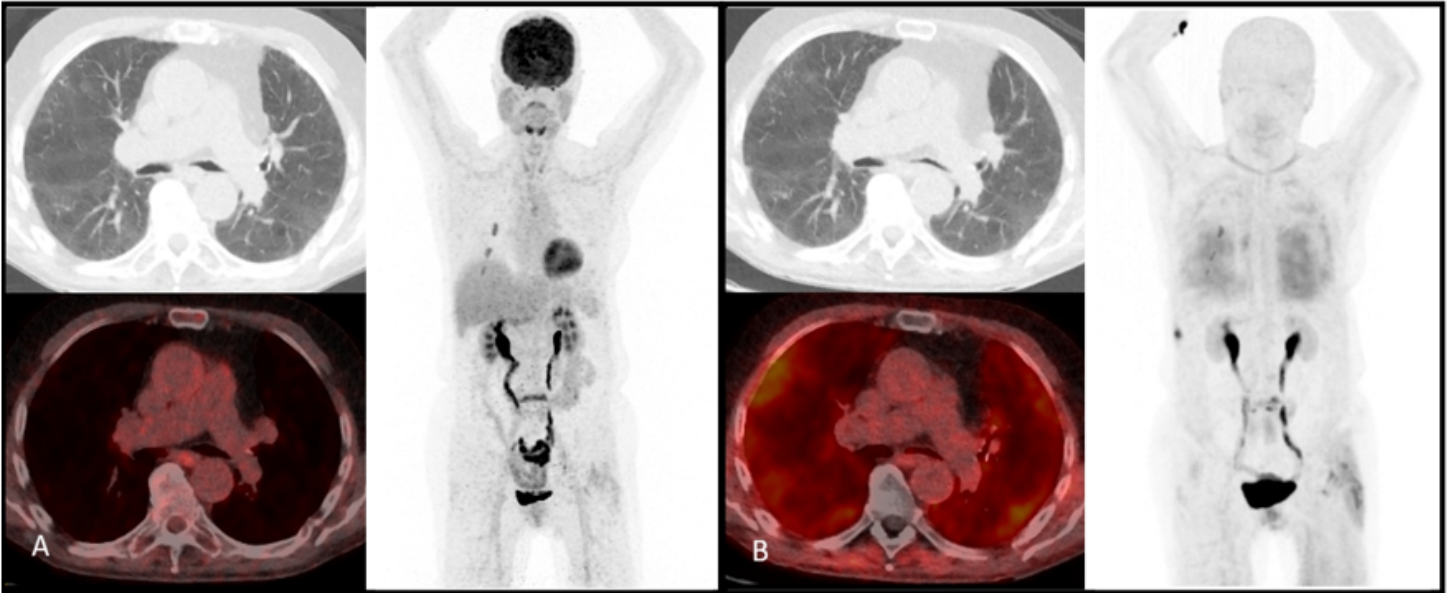


Figure 1

Comparison of transaxial fused positron emission tomography-computed tomography (PET/CT) scans and the respective maximum intensity projection (MIP) with fluorodeoxyglucose (^{18}F -FDG) **(A)** and ^{68}Ga labelled fibroblast activation protein (FAP) inhibitor (^{68}Ga -FAP-46) **(B)**. Showing no relevant accumulation of FDG but an accumulation of FAPI-46, 19 weeks after discharge from hospital, in residual peripheral ground-glass opacities and subtle reticular changes shown in the corresponding low dose CT scans. Additionally, a serial rib fractures rights and inflammatory changes in left hip were detected on both scans.